GO WIDE TO GO DEEP: AFFORDABLE, REPLICABLE ROBOTIC MINIRHIZOTRON SAMPLING FOR PHENOLOGY STUDIES

Richard Nair[1*] / Martin Strube[2] / Martin Hertel[2] / Olaf Kolle[2] / Markus Reichstein[1,3] / Mirco Migliavacca[1,4]

1 Department for Biogeochemical Integration, Max-Planck-Institute for Biogeochemistry, 07745 Jena, Germany

2 Max-Planck-Institute for Biogeochemistry, 07745 Jena, Germany

3 Michael Stifel Center Jena for Data-driven and Simulation Science, Jena, Germany

4 JRC Ispra, Italy

*Corresponding author, rnair@bgc-jena.mpg.de

Keywords: minirhizotron, root dynamics, shoot-root-synchrony, phenocam,

ABSTRACT

1. Minirhizotrons (paired camera systems and buried observatories) are the best current method to make repeatable measurements of fine roots in the field. Automating the technique is also the only way to gather high resolution data necessary for comparison with phenology-relevant above-ground remote sensing, and, when appropriately validated, to assess with high temporal resolution belowground biomass, which can support carbon budgets estimates. Minirhizotron technology has been available for half a century but there are many challenges to automating the technique for global change experiments. Instruments must be cheap enough to replicate on field scales given their shallow field of view, and automated analysis must both be robust to changeable soil and root conditions because ultimately, image properties extracted from minirhizotrons must have biological meaning.
2. Both digital photography and computer technology are rapidly evolving, with huge potential for generating belowground data from images using modern technological advantages. Here we demonstrate a homemade automatic minirhizotron scheme, built with off-the-shelf parts and sampling every two hours, which we paired with a neural network-based image analysis method in a proof-of-concept mesocosm study.
3. We show that we are able to produce a robust daily timeseries of root cover dynamics. The method is applied at the same model across multiple instruments demonstrating good reproducibility of the measurements and a good pairing with an above-ground vegetation index and root biomass recovery through time. We found a sensitivity of the root cover we extracted to soil moisture conditions and time of day (potentially relating to soil moisture), which may only be an issue with high resolution automated imagery and not commonly reported as encountered when training neural networks on traditional, time-distinct minirhizotron studies.
4. We discuss potential avenues for dealing with such issues in future field applications of such devices. If such issues are dealt with to a satisfactory manner in the field, automated timeseries of root biomass and traits from replicated instruments could add a new dimension to phenology understanding at ecosystem level by understanding the dynamics of root properties and traits.

INTRODUCTION

Vegetation phenology (i.e. seasonal patterns of recurrent vegetation events such as leaf growth and seasonal turnover) is one of the main drivers of the interannual variability of the terrestrial carbon sink (Raupach et al., 2011) and a key determinant of vegetation interactions with all biogeochemical cycles both above- (e.g. C fixation, respiration, transpiration) and below- ground, (nutrient and water uptake, respiration). Plant activity is responsive to variation in environmental conditions such as climate and weather (Richardson et al., 2013) as well as species life history strategies and can differ above and below ground (Adair et al., 2019). Thus root and shoot phenology are not always linked (Abramoff & Finzi, 2015; Steinaker et al., 2010; Steinaker & Wilson, 2008) as conditions and resource availability can differ in the two environments (e.g. Blume-Werry, Jansson, & Milbau, 2017) and because plants exhibit intrinsic temporal partitioning of resource uptake, assignment and phenology of individual organs (Herrmann et al., 2016).

Tools to monitor above-ground phenology are well developed, for instance remote sensing techniques such as ‘phenocams’ (e.g. Richardson et al., 2019; Luo et al., 2020) or satellite-derived vegetation indexes (e.g. Wu et al., 2017), but the potential desynchronization of roots and shoots means that using above-ground measurements as a proxy for below-ground activity is at best, an unreliable assumption. Hence phenology relevant measurements of roots are needed in field contexts. Datasets of field root phenology at high resolution are very rare (Radville et al., 2016) because of the demanding and destructive nature of traditional sampling, which also make it impossible to revisit exactly the same spot. This lack of root phenology data contributes to the lack of understanding of the synchronization between above and belowground phenology, and highly simplistic simulation of belowground components growth by models, often relying on poorly calibrated root:shoot ratios, simple environmental triggers, or optimality concepts which are difficult to validate (De Kauwe et al., 2014; Walker et al., 2015).

Apart from plant function, roots are also important for C cycling because they are the main contributor to litter, the control over its decomposition dynamics, and the main C source to SOM pools (Dijkstra et al., 2021) and so misrepresentation of root dynamics at ecosystem scale not only affects understanding of plant function, but of long term ecosystem capacity to sequester carbon. Unfortunately alternative pot and mesocosm experiments are prone to artefacts which disproportionately affect roots (Poorter et al., 2012) so the advantages of field measurements (Schindler, 1998) are even greater for realism belowground. In the field, repeat observations of roots can be made with minirhizotrons (buried observatories and camera

systems, henceforth MRs) since the 1980s (Upchurch & Ritchie, 1984) and in the last decade automation of these systems has been possible (Allen et al., 2007). However, application of such techniques to study field phenology has been very limited and has barely advanced beyond the pioneering experiments using these systems (Allen & Kitajima, 2013, 2014; Iversen et al., 2011; Vargas & Allen, 2008). Current methods use instruments difficult or expensive to deploy in large replication in the field, often due to design specifications for specific problems (e.g. measuring ectomycorrhizal fungi (Allen & Kitajima, 2014) or using the NIR-spectrum to identify dead and living biomass (Svane et al., 2019)). Hence networks of such systems for robust measurements of root dynamics are not in place and nor paired to above-ground measurements. This is also because automatic systems also bring a new bottleneck which severely limits their use – the time taken to manually mark up images.

Automatic interpretation of MR imagery by machine learning is not yet standard and is not the main focus of this paper, but a great deal of image analysis approaches using convolutional neural networks (CNNs) are now being produced to identify roots in a variety of settings (Bauer et al., 2021; Delory et al., 2016; Huo & Cheng, 2019; Rahmanzadeh & Shojaedini, 2016; Vincent et al., 2016). In particular, field minirhizotron imagery has been approached several times with promising results (e.g. Smith et al., 2020; Wang et al., 2019), although the transferability between sites is difficult to assess without widespread adoption of this practice across non-standard instruments (i.e. different cameras between different designs). Without a general model, substantial retraining and benchmarking is necessary on new datasets.

The objectives of this study were twofold: 1) to demonstrate the use of this super-high frequency replicated minirhizotron system (henceforth RMR) with fully analysed observations 2) to show the pairing (or not) between root growth measured with minirhizotrons, shoot growth measured via daily ‘phenocam’ observations and soil respiration fluxes measured with automated chambers in an extremely simple mesocosm. We varied water inputs to mimic an unpredictable growth environment and recorded both the timing of watering and the monitored soil temperatures and shallow soil moisture contents. Our RMR design was made with the constraints of a limited experimental budget. As minirhizotrons have an extremely short field of view (often assumed to be around 2-3mm, but probably actually much shorter (Taylor et al., 2014)), we view affordable replication as a critical element in such attempts to measure in real, heterogenous ecosystems.

For point 1, we captured sub-daily root dynamics in two experiments and processed the images using a CNN method. We validated these data against pixel-level markup. Because these algorithms thus far have not been used in high resolution time series, we were interested in whether it was possible to train a model (with a reasonable amount of effort) which could

accommodate other events which may happen over short time scales not always captured by manual sampling, for example rapid increases in soil moisture content and changes in soil colour following rain (in our case, simulated by precipitation). We used an published segmentation method which performed well in initial trials and assessed its robustness against changing soil moisture, absolute roots in the image and maturity of our experimental system.

For point 2, we tested the following simple hypotheses, starting with ungerminated seeds in the mesocosm:

A) Root development (image indexes from the RMR) would be more sensitive to soil conditions (i.e. water content or temperature) than shoot development (image indexes from the phenocam).
B) However *in general* root development would parallel shoot development during the 2-3 months of the experiment because both indexes are driven by resource availability.
C) CO_2 evolution from the soil (i.e. sum of respiration of roots and microbes) would be linked more strongly to root dynamics than shoot dynamics.

METHODS

Minirhizotron System Design

We based our minirhizotron instrument (RMR) on a movable camera design able to travel in two axes (along a minirhizotron tube, and rotationally around a minirhizotron tube).

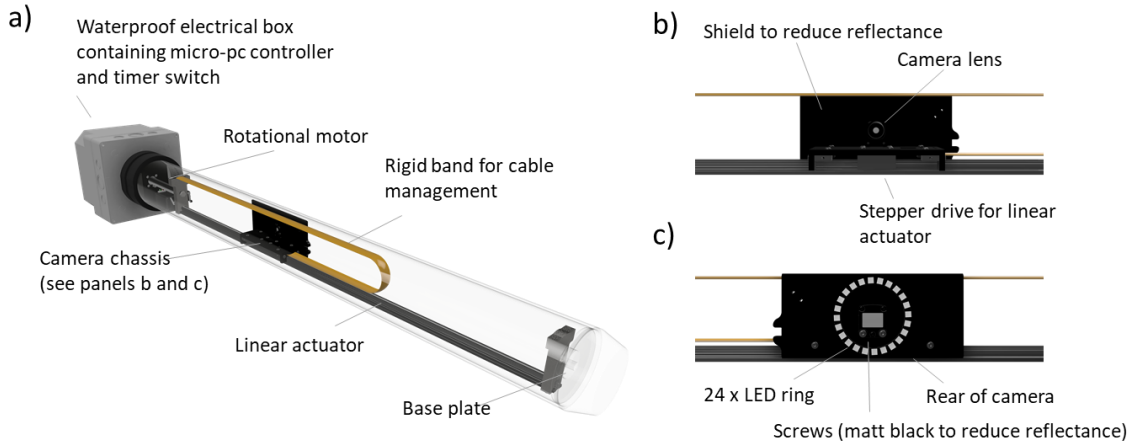

Figure 1. Conceptual diagram of the RMR. The full system (a) moves a camera chassis (b) longitudinally and rotationally to image the soil in close contact with the tube. The camera chassis is designed to minimise reflectance by mounting the light source away from the focal area (c)

The RMR uses a standard RGB digital camera. We changed this camera over the course of the experiments due to supply issues. In Experiment 1 we used an IDS 1005XS-C (IDS imaging Development Systems GmBH, Obersulm Germany). For Experiment 2, we used a DFK AFU050-L34 (TheImagingSource GmBH, Bremen Germany). We used a custom fish-eye lens to allow the camera to focus with a short field of view (~ 3 cm) within the observatory. This had an impact on the field of view (S1) although because we did not expect a meaningful structural distribution of roots on the same scale of individual images we did not correct for this. There was a decrease in image quality in this second system.

The mechanical and electrical components of the RMR were all purchased from suppliers but required some customisation for the precise use case. We used a LattePanda development board computer with integrated Arduino based coprocessor (ATmega32u4, LattePanda, Shanghai, China) and a WiFi antennae to allow remote access. The imaging unit was mounted on a custom-built chassis made of matt black plastic. We used two motors for 360° rotational (NEMA 17 stepper motor with custom 1:49 gear box) and a customized motorized linear rail

system (RGS04K-M0394-A03, Haydon Kerk Motion Solutions, Waterbury CT, USA). This was controlled by the microcontroller alongside a 24 ~4500 k ‘natural light’ led ring (WS2812, Worldsemi, Dongguan, Guangdong, China) which was only switched on when images were taken and was angled away from the image subject to reduce reflectance. All exposed screw heads were painted black for the same purpose. Cable management was achieved by affixing cables to a rigid band only able to bend in the lateral direction. A power supply converter from 12V to 5V was used for the PC, camera and LED ring lights.

We set the timing of sampling through a manual timer switch (RS Pro time switch 1 channel, RS components, Corby, UK) operating the mechanical movement and image capture cycle through shell scripts which ran when the computer successfully booted up and when imaging was complete, shut down the computer. A full sampling cycle takes ~ 40 minutes, covering the entire tube and RMR takes 112 images per cycle, at 8 rotational and 14 lengthwise positions. Images were saved in .jpg formats onto removeable 128 GB SD cards; in order to obtain the images, the SD cards were swapped with blank alternatives during periods when the instruments were not powered. A log file was amended at the end of each imaging cycle which could be checked much faster than individual images and easily accessed over WiFi. A single image was less than 1 Mb, therefore the RMR could sample around 1100 cycles without the SD card being changed.

One sampling cycle from the RMR requires about 10 watt hours of power. Here the RMR ran on mains power, although on occasion was unplugged for several cycles due to other work in its greenhouse location, and/or minor modifications as in this development phase we still had concerns about cable management in the mechanical part of the device. These modifications did not affect the positioning system. The images collected by the RMR overlap by 250 pixels in the lateral direction. For image processing, we trimmed the images to remove overlap so all pixels were independent.

This design of the RMR operates in a 1000 m long x 100 mm (96 mm internal) diameter observatory. This is comparable to the only other automatic minirhizotron systems used in published experiments (Iversen et al., 2011; Svane et al., 2019). The system operates at any angle; generally minirhizotron studies recommend as shallow an angle as possible to minimize artefacts (Cai et al., 2016) or 45° to capture both lateral and horizontal roots (Freschet et al., 2021). The steeper the angle, the deeper the soil an instrument can reach. We also tested the design across a range of temperatures from -20°C to ~ 34°C.

Experiments

We performed two experiments. Experiment 1 (E1) used a single RMR, Experiment 2 (E2) used 8 replicated RMRs. Aside from the camera used, which we changed due to uncontrollable supply issues, the design was the same with the exception of minor modifications for cable management (also detailed later). CO_2 fluxes were measured in E1. The objectives of the experiments were, in a greenhouse context, 1) to test the systems (E1 and E2) 2) demonstrate the potential for linkage of high resolution above-ground biomass and root phenology data (E1 and E2) 3) along-side soil CO_2 flux evolution (E1) and 4) to demonstrate the consistency between multiple instruments both in terms of instrument performance and application of a single trained neural network to segment all images (E2).

We used up to eight RMRs, each located in a 1 m observatory. Each observatory was located horizontally in a 140 cm (L) x 40 cm (W) x 30 cm (H) mesocosm unit. The length of the observatory extended 100 cm from one end of the mesocosm, the RMR is designed for field operation which is usually at an angle so the first ~ 10 cm of the length, which are usually partially above ground were not sampled. Each mesocosm was filled with sieved soil (roots and stones removed via sieving to 0.5 cm), harvested from Meusebach, Thuringia Germany (originally a dystric cambisol, L. Eder pers. comm.). C:N of the soil was 18:2.The soil column in each mesocosm ended 2 cm above the upmost surface of the minirhizotron; because of the horizontal installation, the minirhizotron field of view spanned between 2 and 12 cm below the soil surface.

Soil in the mesocosm units was smoothed with hand tools and in both experiments planted with a 3-species seed mix (80 % *Anthroxanthum odoratum, 15 % plantago lanceolata,* and 5 % *Medicago scutellata* by mass). These were scattered evenly over the surface of the mesocosm and kept moist to germinate on the soil surface. Water was provided at irregular but recorded intervals and volumes via a watering can with a distributor nozzle. We applied water sufficient to sustain a growth response until an arbitrary point in the development of each mesocosm, then we withheld water to encourage the system to proceed towards a state of (drought induced) root senescence, allowing a further assessment of the robustness of the segmentation algorithms applied. This period was longer in Experiment 2 (1 month) than Experiment 1 (2 weeks).

Secondary Installation

All mesocosm units used in both experiments were included in the field of view of a standardised ‘phenocam’ (Richardson et al., 2018; Sonnentag et al., 2012) NIR-infrared enabled digital camera (StarDot NetCam 5MP, StarDot Technologies, USA), which we

modified for indoor installation by equipping with a fish-eye lens (StarDot LEN-3.6MMCS, StarDot Technologies, USA)to widen the field of view. The camera settings were defined from the 'PhenoCam' protocol (Richardson et al., 2018). Images were collected between midday and 1pm local time. During this time artificial lights were switched off and watering was never during this hour. FOVs during each experiment were stable and images were available from the entire period. We extracted the Green Chromatic Coordinate (GCC), that is the ratio between the mean value of the digital numbers of the green channel divided by the sum of the reg, green, and blue channel (Gillespie et al., 1975), for the region of interest (ROI) in the image. We defined a single ROI for each entire mesocosm unit, parallel to the long axis of the minirhizotron. Data was processed as in field-scale studies (e.g. Luo et al., 2018, 2020). GCC is a measure of greenness to overall image brightness commonly used in phenocam studies to represent canopy structure. It has been found to outperform NDVI in forests when assessing vegetation cover and condition and supressing scene illumination variation (Nijland et al., 2014). Using greenness indexes relies on the assumption that healthy vegetation is greener and less healthy vegetation is less green.

We measured soil properties, a combination of EC-5 soil moisture probes (Li-COR Biosciences, USA) and ML-3 soil temperature probes (Decagon Instruments, USA), all installed on the soil surface, sampling the top 0-5 cm soil. We also made destructive 'ground truthing' of roots. We installed six 4.5 cm, 13 cm deep ingrowth cores in each mesocosm. These were evenly spaced, at 5 cm from the wall of the unit and an equal distance from the central minirhizotron tube. These were retrieved and root biomass measured by sieving the soil to 2 mm and weighing the washed and dried (60°C, 3 days) roots. In E1, we sampled six unreplicated (to minimize disturbance and because of the limited area of soil not occupied by the minirhizotron or the gas exchange measurement) time points plus the start (no roots), while in E2 we sampled the start (no roots), three unreplicated time points, and then one time point at the end of the experiment with 3 replicates per mesocosm.

We also measured 'system' gas exchange using a Li-8100A IRGA, a Li-8150 multiplexer, and a Li-8100-104 opaque long-term chamber (Li-COR Biosciences, USA) every half-hour. We let vegetation grow within the chambers. These data were processed using the R package RespChamberProc; in general the fit of all observations was very good (< 99% with an R2 of 0.99).

Experiment 1

In E1 we operated a single RMR, measuring every two hours from mid September to mid December 2018. We sampled around 690 cycles in this period with occasional periods of power disruption, for 75000 total images.

Experiment 2.

In the E2 we ran a RMR in each mesocosm (eight in total) every six hours from Mid-July to Mid-September 2019. The full dataset for this experiment contained 216,000 individual images.

Processing of Minirhizotron Imagery

Processing automatically sampled data streams

All pre-processing (image cropping) and image segmentation was conducted in Python 3. For root image segmentation (i.e. separation of the root image pixels into two classes, roots and soil), we trained a CNN (convolutional neural network)-based model with a GUI allowing corrective annotation (*Rootpainter*, Smith et al., 2020) on each experiment separately. We started with a random model and without any pre-annotated images, on 308 complete 2292 x 1944 pixel images for E1, and 300 images for E2, stopping when we (qualitatively) assessed the segmentation was not improving. We validated segmentation of the images in E1 against 384 unseen fully annotated images (but not used to train these algorithms) by annotating the images using GIMP software (The GIMP Development Team, 2019) to the pixel level. This data covered the full period of the experiment but was biased in terms of data towards the first month. For E2, we validated these against 240 manually annotated images. In both cases the images were manually annotated by multiple users with randomized filenames to prevent prior knowledge affecting mark-up. In this experiment we both changed the camera used due to supply issues and re-used the experimental set up following a previous non-automated experiment where emptying and re-filling the mesocosms had left minor scratches and impressions (likely caused by exudates or sloughing of dead cells) of previous roots on the tube surface which were not visible to the naked eye on the soil-free tube but could be seen by the minirhizotron images with dark contrasting soil background. While we could reasonably successfully train the model to distinguish between roots and scratches, this introduced a large source of error between this and human annotation and so we acknowledge that errors would arise in E2 due to ambiguity about root locations.

We chose to use the simple percentage cover of roots in our image as our metric of analysis. We did this for several reasons. First, it was easy to train for, meaning we needed less good quality annotations to predict this well with the CNN. Second, we were already using an image index for above-ground measurements and considered another coarse metric acceptable for comparison. Thirdly, it was also easier to produce good quality validation data simply for image pixels without needing full or connective annotation of individual roots. We calculated the percentage cover of roots in the segmented images. After considering these data between images, we realised that the horizontal installation meant that images on the top of the tube were different than at the bottom (see S3). After consideration of this, we treated the top of the tube as 'truth' and used this 3/8 of a complete rotational series for further data analyses.

Data analysis:

We observed a weak sub-daily cycle in the roots identified, especially later in the time series. This was because of an artefact which affected root identification, particularly on the sides of the observatory (see S2) which was not caught by our validation procedure. Based on our knowledge of what the model was segmenting (biomass, which should not change on these scales), this artefact clearly affected the segmentation, rather than what actually *was* roots in the soil. Hence, we averaged over each calendar day for a single daily 'cover' value. We then performed a further rolling average for 3 days in common with other field phenotyping approaches above-ground (e.g. Aasen et al., 2020). To calculate growth rates, we took the linear slope in this average over a 5 day window.

In order to analyse the overall model accuracy and usefulness as a replacement for manual annotation for root cover, we used R (R Core Team, 2018), using the lmodel2 package (Legendre, 2018) for reduced major axis regressions, in order to account for the similar error in the x (manual annotated root cover) and y (neural network classified root density) dimensions. We used linear regressions to compare the differences between the manual and neural network classifications and if a systematic bias was introduced by potential confounding variables such as time, soil water content, and the absolute number of roots in the image. To analyse the effects of mesocosm conditions on CO_2 efflux in Experiment 1, we fit a GAM (generalized additive model, Hastie & Tibshirani, 1986), implemented via the mgcv package in R (Pedersen et al., 2019), which allowed an independent, non-linear smooth to be fit for each predictor. For predictor variables, we used normalized soil moisture content, temperature, the 5-day slope of normalized root cover and normalized GCC and the relative total GCC, fitting a univariate smooth for each predictor without interactions. We did not use the relative root cover due to the very high concurvity between this and GCC. Otherwise, concurvity in all cases was less than 0.7. The GAM approach was appropriate because we

did not necessarily expect the relationships of the predictors to the soil CO_2 flux to be linear (e.g. more soil respiration could occur due to root growth (positive slope) or root turnover (negative slope). We compared the variable importance in these models using the varIMP function in the caret package (Kuhn, 2008).

RESULTS

We successfully collected and processed imagery both above- and below- ground, allowing us to validate this against manual annotation and interpret the relationships between above-ground growth (GCC) and below ground growth (root cover).

<u>Experiment 1:</u>

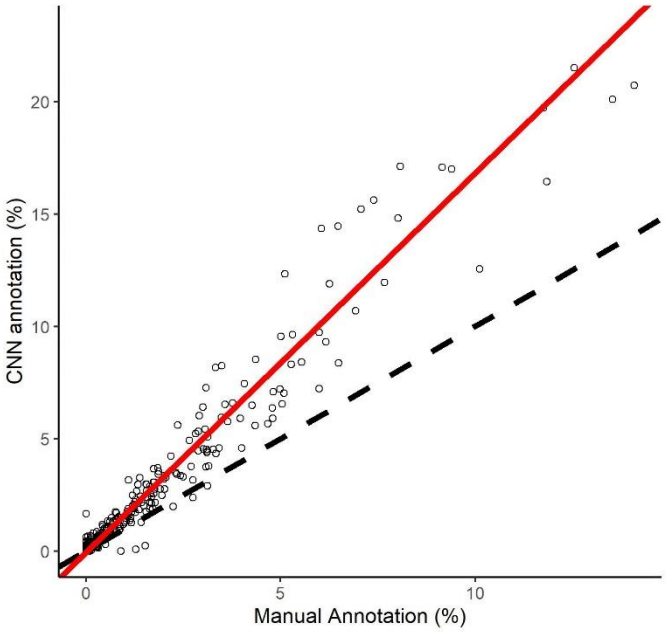

Figure 2. Validation of CNN-annotation against independent manual root annotation. The red line shows a reduced major axis regression of the two variables, while the dashed line is a 1:1 relationship.

We achieved a R2 of 96 % in terms of pixels identified as roots in the unseen annotated images (Figure 2). The model identified significantly more pixels as roots ($P < 0.01$) than human annotation. In addition, while there was an expected relationship between manual cover and the absolute difference between CNN and manual markup (bigger values could be more wrong, figure 3a), there was no effect of time, measured soil moisture content or manual cover on the error relative to the manual cover (figure 3b, 3c, 3d). This indicated that we could trust the segmentation on average over the whole time series.

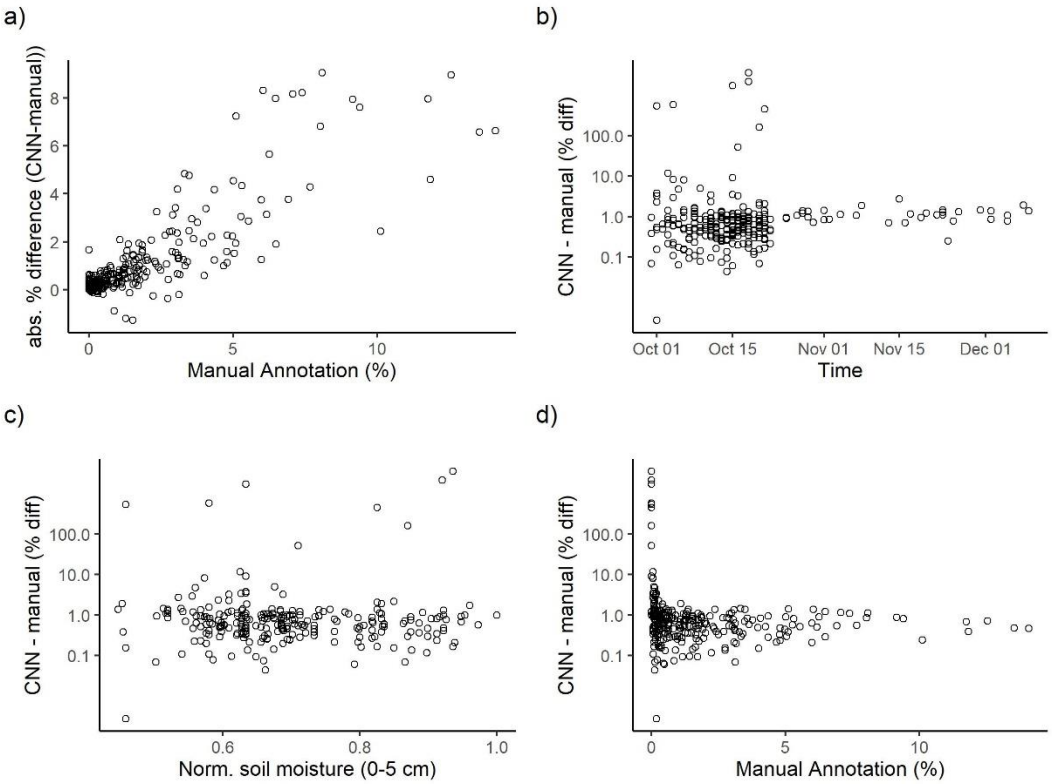

Figure 3. a) absolute percentage difference between manual annotation and CNN-classified pixels b), c), d) relative percent difference standardised to manual annotation over b) time, c) soil moisture content in the 0-5 cm soil at time of sampling and d) manual cover. Only the increased absolute error at higher levels of manual cover was significant (which was expected). The clustering of data towards the early part of panel b is due to an uneven production schedule.

We also examined the entire time series of CNN-segmented data.. We could pair this time series with the time series from GCC and the absolute root mass measurements (Figure 4 a.). We also found a good match between absolute root mass and root cover (although the former was un-replicated). Interestingly, when compared to the total amounts of water applied, some of the instability in root cover appeared to be related to the watering events late in the mesocosm, where identified root cover notably dropped in the period following watering, a potential water effect not caught by comparison with SWC (Figure 4 a).

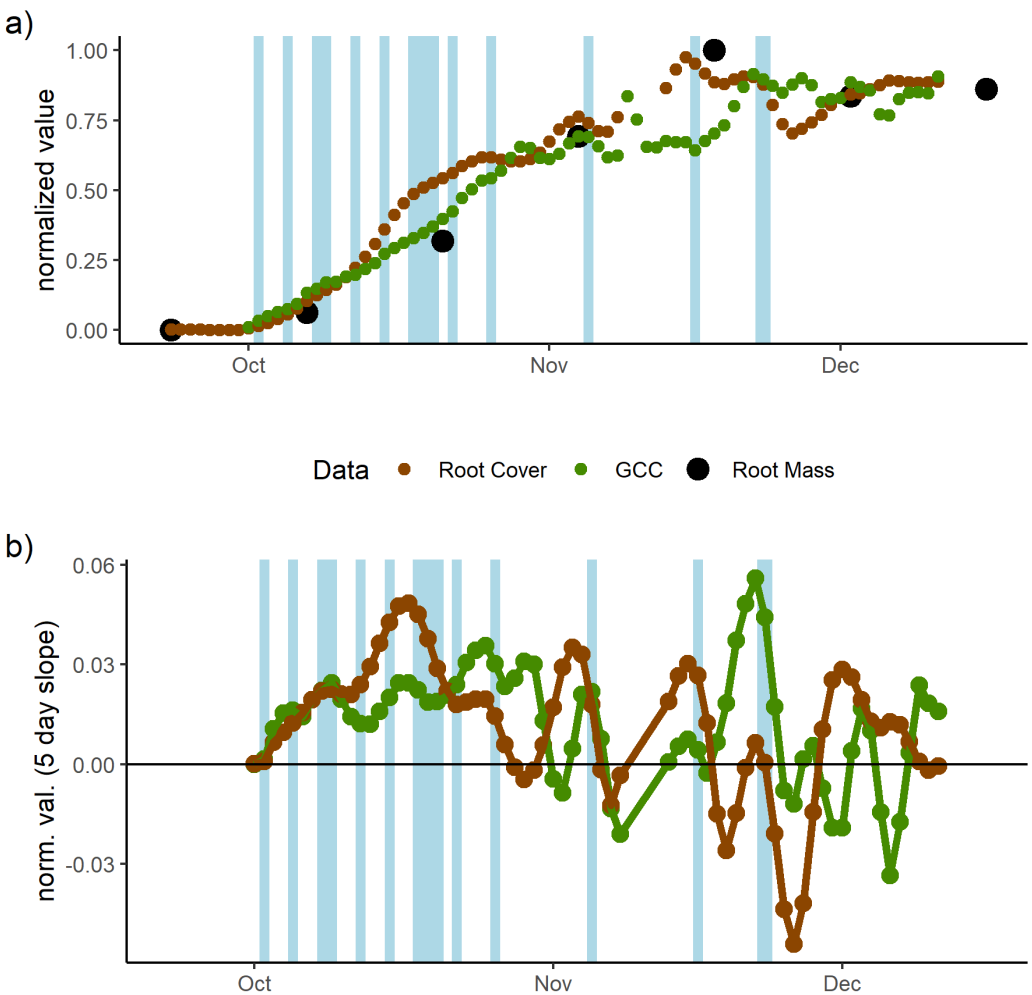

Figure 4. A time series of root data from the mesocosm experiment. Panel a) shows the relative, 3-day smoothed root cover, GCC, and root mass showing parallel development. Panel b) shows the 5-day slope of these values (i.e., rate of change) where at some periods GCC is increasing faster than root cover and at others root cover is increasing faster than GCC. Blue lines show watering events which are scaled in width relative to the volume of water applied.

We were also able to compare the rates of change. In general, this 5-day slope differed between the two indexes (figure 4b) except at the start of the experiment. As previously mentioned, from around the start of November there was a decrease in the root index (and sometimes the GCC following watering). The root cover index continued to be positive at the end of the experiment even when the GCC was stable or decreasing as the soil slowly dried out.

When we fit the GAM model to Experiment 1, we were able to explain 68% of the total variation in CO_2 soil efflux with the best fitted model (Figure 6 a). In this model, soil moisture content (P

< 0.001) GCC ($P < 0.05$), the slope of root cover ($P < 0.001$), and the slope of GCC ($P < 0.05$) were all significant. Root growth (slope_cover) and not biomass itself (GCC, which correlated strongly with root cover) was the most important variable in determining soil CO_2 efflux (Figure 5 b) and increasing root growth rate had a positive effect on soil CO_2 efflux (Figure 5 d). Notably, negative root growth rates had no effect whereas negative GCC slopes, our proxy for leaf growth rate, did, although both smaller overall effect and more dispersed partial residual of the GCC slope meant this was a far worse determinant than root growth rate on soil CO_2 efflux

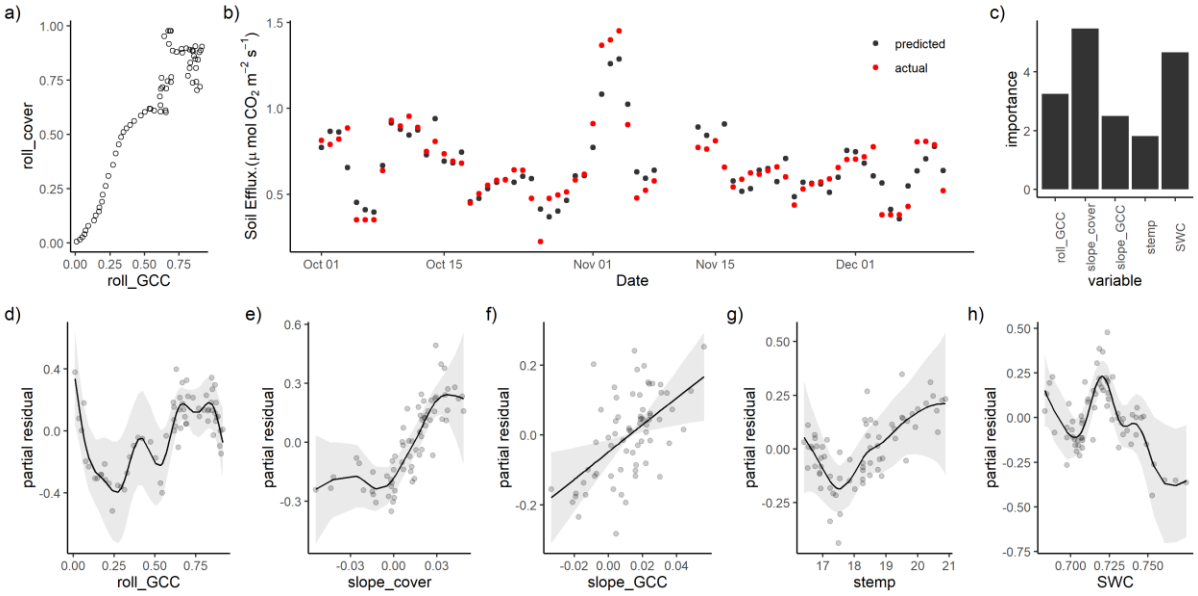

Figure 5. Summary of the GAM model fit for E1. Root cover (roll_cover) correlated with GCC (panel a) so we only used GCC in the main model. We were able to predict the daily CO_2 flux fairly well with an R_2 of 68% (panel b). The model contained univariate smooths for rolling GCC (roll_GCC, shown vs partial residuals in panel d), the 5-day slopes (i.e. growth rate) of root cover (slope_cover, panel e) and GCC (slope_GCC, panel f), soil temperature (stemp, panel g) and soil moisture content (SWC, panel h). Shaded area shows 2 x SE. When variable importance was considered (panel c), the slope of root cover (i.e. change in amount of roots, birth or death) was a much better predictor than that of above-ground GCC.

<u>Experiment 2:</u>

We did not achieve such as good fit against manual annotation in E2 (R2 = 72 %), but as already discussed, the images here were of considerably worse quality. Overall, a similar time series was extractable from each mesocosm (Figure 5). Correlation between GCC and root cover was between 0.7 and 0.96 (Figure 6). Notably, the mesocosms were arranged in

numerical order and GCC increased faster than root cover in the first four mesocosms, suggesting that a gradient (e.g. light) within the greenhouse may have driven a difference.

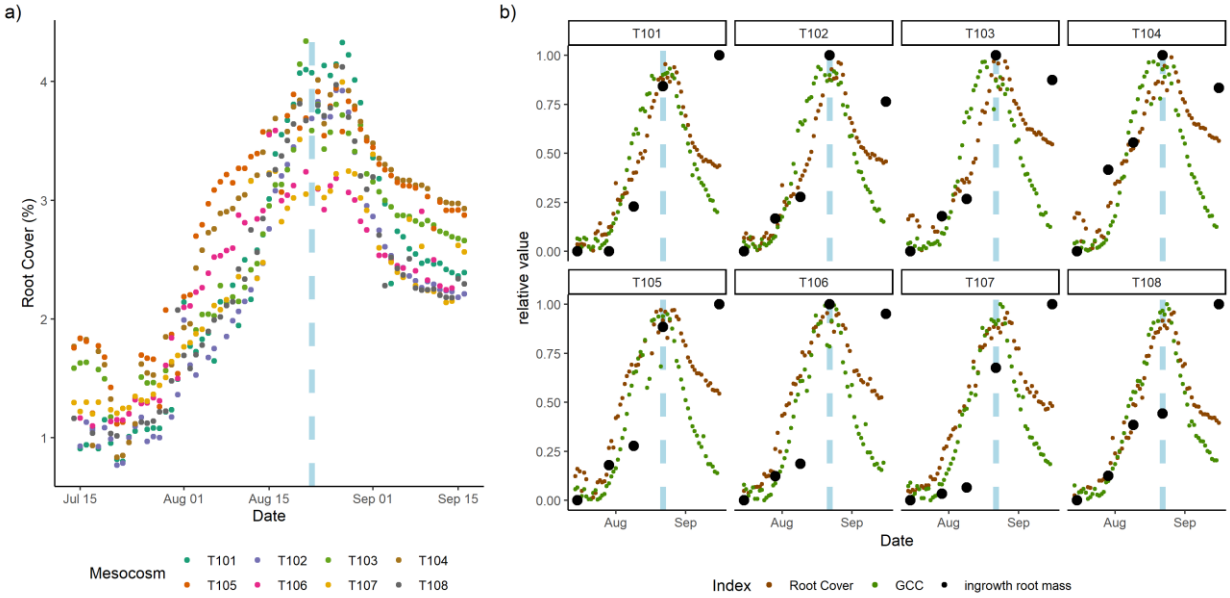

Figure 6: a) Comparison of absolute root cover from all mesocosm units. Absolute difference in root mean cover was around 1 % of the total image or 25 % of the total area covered b) Comparison of GCC and root cover from all 8 mesocosm units. GCC matched root cover well in all cases and both indexes peaked after watering finished (blue line in both panels). In most mesocosms GCC reached its maximum before root cover. Generally, the both the mismatch between root cover and ingrowth root mass and the match between root cover and GCC with root cover was worse at the end of the experiment.

The roots extracted from the ingrowth cores at the start of the experiment matched the overall time series (when normalized between mesocosms). However, the last data point, collected at harvest did not, and the measured root biomass was still high when the root cover index had dropped. Once watering ceased, root growth rate remained positive for longer than GCC growth rate (Figure 6), indicating a continued production of these organs even as the above-ground began to yellow.

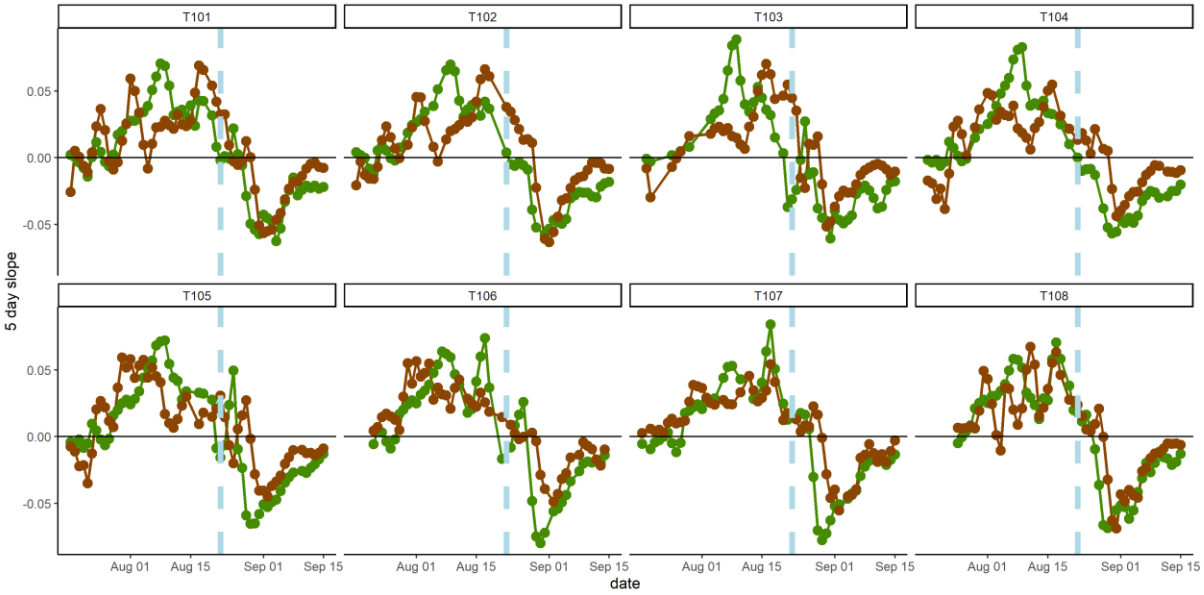

Figure 7. 5-day slope (growth rate) of above- and below-ground indexes across 8 mesocosms. Vertical blue line indicates the last watering date, horizontal black line is 0 and the transition point between positive growth rates (above-) and a decrease in the index (below-) indicating yellowing or disappearance of roots identified by the CNN trained on 'living' roots.

DISCUSSION

<u>Use of automatic minirhizotrons to generate high resolution root data</u>

The minirhizotron (MR) technique balances the ability to repeatedly measure fine roots in the field with limited bias if installed well, and is the best method to measure phenological properties of roots (Freschet et al., 2021). Automation of the whole workflow, from image collection to analysis is essential to make high time resolution data available. While huge steps have been previously made in image collection (e.g. Allen & Kitajima, 2013), these have both not been deployed at large field scales as part of an automated workflow. Because of constraints mentioned in the introduction of this paper (cost of replication, image volume and analysis time for human interpretation), there has been no work pairing indexes of root data on the same scales as above ground vegetation indexes useful for whole system phenology interpretation.

Here we presented a newly built MR system, capable of image capture at up to the hourly scale, and demonstrated a fully automatic operation in a controlled greenhouse setting. Our systems could sample in less than an hour, and were constructed on a relatively low budget (around 2000 euro for materials), which allowed us to construct multiple instruments, and

produced similar data sets from replicated mesocosms despite independent sensors (Figure 4). Methods such as phenocams have already achieved standardisation using a single instrument, but automatic minirhizotrons need to combine robotics and imaging sensors, which are both rapidly advancing fields. There are also a large number of potential questions at the more local minirhizotron scale, requiring different levels of magnification and sampling time, as well as demands on power supplies. Hence, we recommend against a standardisation of such designs if time and expertise is available to build home-made instruments. Imaging properties differ between cameras, but minirhizotrons must be validated regardless (ideally against both annotated images and biomass or the traits in question) and the property of interest always requires image interpretation.

Our approach aimed to replicate as far as possible on a limited experimental budget. Replication is a key shortcoming of many field studies (Filazzola & Cahill Jr, 2021; Yang et al., n.d.) and is especially important for minirhizotron studies given the short field of view of such instruments, numerous potential artefacts from MR devices (Joslin & Wolfe, 1999) and huge range of soil and root appearances. We also fully analysed our data using an automated method. While we discarded 5/8 of the rotational series even in our most thorough analysis due to the position of the minirhizotron, this represents to our knowledge the largest ever MR image set per time ever analysed. Data collected at such high resolution has multiple issues which we encountered in this simple analysis with implications for application of such techniques to more complex situations in the field. Therefore, the majority of this discussion concerns these issues.

<u>Interpreting High Resolution Root Image Data</u>

Neural-network based methodologies are an obvious approach to analysing MR images and follow the recent vast advances in phenotyping in other fields of root biology (Atkinson et al., 2019). We applied an off-the-shelf segmentation algorithm (Smith et al., 2020) for root images. We chose this method because of the advantages offered by a simple GUI for corrective annotation. This method for training data generation offers major advantages for minirhizotron annotation in mixed field communities where root appearances may vary, because problematic features can be quickly selected for training. For the purpose of this study this method performed well, we had a high correlation in total root pixels annotated in the images (Figure 2). We chose this metric because we were comparing with a similarly coarse above-ground index. In total, our training took about 2 person-days for each experiment. Our images also featured other artefacts including scratches to the observatory surface from earlier system tests which we were able to train the model to avoid, but may have slowed fitting. Nonetheless, enough appropriate training data is a major issue for automatic minirhizotron studies which do

not suffer from (unintentional) observer bias in environmental conditions inherent in manual sampling, i.e. potentially missing periods immediately after rain and with only short intervals between images. Issues with these short-term changes were apparent in our data and visible once roots were established in Figure 4. In practice, coping with these events is very difficult across large datasets because random validation data is unlikely to capture these events and targeting these times introduces bias. Thus, high throughput of training data offers one major advantage in such unpredictable tasks over dense annotation strategies.

Automatic instruments paired with automatic root identification are demanding on training data to cope with variable field conditions but also reliant on validation to give useful information. In this study we were able to use fully segmented images produced for other neural network trials as one form of validation data. It is important to note that in this context such images are human-best practice annotation and may be outperformed both consistency and accuracy in identifying the true properties of interest by an appropriately trained neural network. For global change studies, where above-ground vegetation indexes are similarly coarse in space and time (e.g. 3-day averaging phenocam data (Aasen et al., 2020)), a similar accuracy as experiment 1 (96%) or even experiment 2 (72%) is sufficient for generating plausible time series (eg. Figure 4b, Figure 6), relatable to function (Figure 5). Indeed, from our simple modelling approach, change in root cover proved a more important predictor of soil carbon fluxes than change in the greenness of the plant canopy.

In Experiment 1, we also found a surprisingly good correlation in physical validation between root mass and minirhizotron root cover, which was also supported by the growth period of Experiment 2 (but not the last, replicated measurement, discussed later). While the whole rationale of our instrument is that mesocosm experiments are *not* good replacements for field root measurements (Poorter et al., 2012) some further consideration is due to using minirhizotrons for dynamic biomass pools. While there are differences in the properties actually measurable from minirhizotrons and other methods in many systems (e.g. Addo-Danso et al., 2016; Milchunas, 2009; Nair et al., 2019), minirhizotrons are a reasonable index of biomass if appropriate conversions are applied (e.g.Brown et al., 2009; Johnson et al., 2001; Lee et al., 2017; Sullivan & Welker, 2005). Indeed, identification of roots relates directly to meaningful biological structures in a close to 2D surface around a minirhizotron observatory. This can potentially be paired far more easily with density and carbon contents than leaf greenness indexes of a whole canopy, if the short range of the instruments can be offset by sufficient replication. A key aspect of future studies with automatic minirhizotrons will be to ascertain whether well-known artefacts of roots in minirhizotrons (Rytter & Rytter, 2012; Vamerali et al., 2009) can be understood enough to correct for these issues, and indeed if

potential artefacts such as root growth differences interact with seasonal cycles and environmental conditions.

A further issue with our CNN-based annotation of the automatic MR images related to unrealistic variation in the root pixel identification which occurred both after watering events (Figure 4) and between different hours of the day (Figure S2). Like similar issues when using classifiers for data from NIR-enabled minirhizotrons (Svane et al., 2019) sudden changes in soil colour/reflectance led to erroneous pixel-wise identification and subsequent unrealistic changes in overall root identification. Interestingly for the sub-daily data, the similar issue is not explainable due an effect of soil moisture content from the surface sensors (Figure 2 c.), which could be because effects at the minirhizotron surface (which could include very local condensation) were not represented by our surface soil moisture measurement. Indeed, the effect of sub-daily variation only became apparent in both mesocosm experiments after roots had colonized the sides of the observatories, which suggested that the CNN was not misidentifying pixels in general, but pixels in close proximity to roots. Inspection of the root images confirms this explanation (Figure S2). Hydraulic redistribution (passive movement of waster via roots from areas of wetter to drier soil, (Ryel, 2004) at night and transpiration during the day wetting and drying these roots may provide an explanation for these effects which may bias a segmentation model more than human annotation. If this affected the immediate 'rhizosphere' only, this would not have been detected by our soil moisture content sensors.

There are several potential solutions to this issue. The first is to aggregate, smooth or throw out data at sufficient timescales to remove such effects, which disregards a large amount of the information from high resolution sampling but is common practice at ecosystem level e.g. using smoothing splines (e.g. Migliavacca et al., 2011 on PhenoCam data) However if one wants to analyse sub-daily data (as may be the case for many short term events and interpret the difference between immediate successive image samplings) this is not a good solution. Secondly, a data handling approach could post-process with human intervention, applying an adjustment or a separately trained model to periods with problematic changes in soil appearance. Such an approach is also not favourable because of the need to interfere with the image index. Thirdly, effort can be made to train on more data, particularly around periods of difficulty. This would require more training time, especially if randomly selecting data and if problematic events are rare but important. Fourthly, consistency in pixel-wise annotation between sequential images could be used as a filter for 'true' observations, if true changes during a period of instability in the index are unidirectional (i.e. basing interpretation on objective priors about root growth patterns). Finally, a wholly different model structure incorporating either a reliance on other factors such as soil moisture (which may be indicative of times when this could occur even if it does not proscribe events at the root-tube interface)

or time series information (e.g. via recurrent network architectures such as Long-Short Term Memory approaches (Hochreiter & Schmidhuber, 1997), multivariate time series classification (Ruiz et al., 2021) or other time series classification approaches (Fawaz et al., 2019)) could be built. This has the advantage of processing all data from automatic minirhizotrons without bias (if training data is selected fairly) at the cost of a more complex model structure and/or more variables to measure alongside root imagery.

Relevance for Ecology and Carbon Cycling Knowledge

While the experiments described herein were primarily to test an automatic minirhizotron system, we can also consider the knowledge gained from these approaches. We observed an apparent de-synchronicity in the short term from our two image indexes, indicating that development of roots and shoots, as observed by our methods, was not in sync (Figure 4b, Figure 7). This matches some conventional studies which suggest that even in short stature vegetation asynchrony may occur (Sloan et al., 2016; Steinaker et al., 2010; Steinaker & Wilson, 2008). It is important to note that this was not a field experiment and we were not measuring true phenology, rather development from seed and so care must be taken in applying any conclusions to a wide scale. However, in our case, this asynchrony was happening on an extremely short scale of several days. Such fine distinctions potentially have impact on the interpretation of C uptake and respiration in real field experiments and should be tested in these contexts. From the modelling exercise in Experiment 1, change in roots also were a better indicator of soil CO_2 evolution than leaf greenness and from our root biomass measurements, the minirhizotrons were a reasonably proxy for the root biomass. Hence with appropriate calibration data automatic minirhizotron imagery could be interpreted as changes in C pools. Interestingly the ‘harvest’ data point in experiment 2 did not match the minirhizotron index, even when scaled. This is potentially explainable by the CNN, trained on live roots, being better at distinguishing between living and dead biomass than human operators sorting physical samples. A further development of such methods, e.g. training models specifically on dead roots, using multi-classifier segmentation or generating labels using NIR or other spectral images (Arnold et al., 2017; Bodner et al., 2017) and segmenting using RGB images may be a way to achieve this distinction in the field datasets necessary for quantification of root biomass and its complex and dynamic contribution to ecosystem C cycling.

ACKNOWLEDGEMENTS

This project has received funding from the European Union's Horizon 2020 research and innovation programme under the Marie Sklodowska-Curie grant agreement No. 748893 (Marie Sklodowska-Curie Individual Fellowship to Richard Nair). We also thank Marion Schrumpf for her very useful comments on this manuscript.

BIBLIOGRAPHY

Allen, M. F., & Kitajima, K. (2014). Net Primary Production of Ectomycorrhizas in a California Forest. *Fungal Ecology*, *10*(1), 81–90. https://doi.org/10.1016/j.funeco.2014.01.007

Allen, M. F., Vargas, R., a. Graham, E., Swenson, W., Hamilton, M., Taggart, M., Harmon, T. C., Rat'Ko, A., Rundel, P., Fulkerson, B., & Estrin, D. (2007). Soil Sensor Technology: Life within a Pixel. *BioScience*, *57*(10), 859. https://doi.org/10.1641/B571008

Arnold, T., Leitner, R., & Bodner, G. (2017). Near infrared hyperspectral imaging system for root phenotyping. *Sensing for Agriculture and Food Quality and Safety IX*, *10217*, 94–99. https://doi.org/10.1117/12.2262441

Atkinson, J. A., Pound, M. P., Bennett, M. J., & Wells, D. M. (2019). Uncovering the hidden half of plants using new advances in root phenotyping. *Current Opinion in Biotechnology*, *55*, 1–8. https://doi.org/10.1016/j.copbio.2018.06.002

Blume-Werry, G., Jansson, R., & Milbau, A. (2017). Root phenology unresponsive to earlier snowmelt despite advanced above-ground phenology in two subarctic plant communities. *Functional Ecology*, *31*, 1493–1502. https://doi.org/10.1111/1365-2435.12853

Bodner, G., Alsalem, M., Nakhforoosh, A., Arnold, T., & Leitner, D. (2017). RGB and Spectral Root Imaging for Plant Phenotyping and Physiological Research:

Experimental Setup and Imaging Protocols. *Journal of Visualized Experiments : JoVE*, *126*, 56251. https://doi.org/10.3791/56251

Brown, A. L. P., Day, F. P., & Stover, D. B. (2009). Fine Root Biomass Estimates from Minirhizotron Imagery in a Shrub Ecosystem Exposed to Elevated CO2. *Plant and Soil*, *317*(1–2), 145–153. https://doi.org/10.1007/s11104-008-9795-x

Cai, G., Vanderborght, J., Klotzsche, A., van der Kruk, J., Neumann, J., Hermes, N., & Vereecken, H. (2016). Construction of Minirhizotron Facilities for Investigating Root Zone Processes. *Vadose Zone Journal*, *15*(9), 0. https://doi.org/10.2136/vzj2016.05.0043

Delory, B. M., Baudson, C., Brostaux, Y., Lobet, G., du Jardin, P., Pagès, L., & Delaplace, P. (2016). ArchiDART: An R Package for the Automated Computation of Plant Root Architectural Traits. *Plant and Soil*, *398*(1–2), 351–365. https://doi.org/10.1007/s11104-015-2673-4

Dijkstra, F. A., Zhu, B., & Cheng, W. (2021). Root effects on soil organic carbon: A double-edged sword. *New Phytologist*, *230*(1), 60–65. https://doi.org/10.1111/nph.17082

Filazzola, A., & Cahill Jr, J. F. (2021). Replication in field ecology: Identifying challenges and proposing solutions. *Methods in Ecology and Evolution*, *12*(10), 1780–1792. https://doi.org/10.1111/2041-210X.13657

Hastie, T., & Tibshirani, R. (1986). Generalized Additive Models. *Statistical Science*, *1*(3), 297–310. https://doi.org/10.1214/ss/1177013604

Herrmann, S., Grams, T. E. E., Tarkka, M. T., Angay, O., Bacht, M., Bönn, M., Feldhahn, L., Graf, M., Kurth, F., Maboreke, H., Mailander, S., Recht, S., Fleischmann, F., Ruess, L., Schädler, M., Scheu, S., Schrey, S., & Buscot, F. (2016). Endogenous rhythmic growth, a trait suitable for the study of interplays between multitrophic interactions and tree development. *Perspectives in Plant Ecology, Evolution and Systematics*, *19*, 40–48. https://doi.org/10.1016/j.ppees.2016.02.003

Huo, C., & Cheng, W. (2019). Improved root turnover assessment using field scanning rhizotrons with branch order analysis. *Ecosphere*, *10*(8), e02793. https://doi.org/10.1002/ecs2.2793

Iversen, C. M., Murphy, M. T., Allen, M. F., Childs, J., Eissenstat, D. M., a. Lilleskov, E., Sarjala, T. M., Sloan, V. L., & Sullivan, P. F. (2011). Advancing the Use of Minirhizotrons in Wetlands. *Plant and Soil*, *352*, 23–39. https://doi.org/10.1007/s11104-011-0953-1

Johnson, M. G., Tingey, D. T., Phillips, D. L., & Storm, M. J. (2001). Advancing fine root research with minirhizotrons. *Environmental and Experimental Botany*, *45*(3), 263–289. https://doi.org/10.1016/S0098-8472(01)00077-6

Joslin, J. D., & Wolfe, M. H. (1999). Disturbances During Minirhizotron Installation Can Affect Root Observation Data. *Soil Science Society of America Journal*, *63*(1), 218–221. https://doi.org/10.2136/sssaj1999.03615995006300010031x

Lee, C. G., Suzuki, S., Noguchi, K., & Inubushi, K. (2017). Estimation of Fine Root Biomass Using a Minirhizotron Technique among Three Vegetation Types in a Cool-Temperate Brackish Marsh. *Soil Science and Plant Nutrition*, *62*(5–6), 465–470. https://doi.org/10.1080/00380768.2016.1205957

Legendre, P. (2018). *lmodel2: Model II Regression* (1.7-3) [Computer software]. https://CRAN.R-project.org/package=lmodel2

Luo, Y., El-Madany, T., Ma, X., Nair, R., Jung, M., Weber, U., Filippa, G., Bucher, S. F., Moreno, G., Cremonese, E., Carrara, A., Gonzalez-Cascon, R., Escudero, Y. C., Galvagno, M., Pacheco-Labrador, J., Martín, M. P., Perez-Priego, O., Reichstein, M., Richardson, A. D., … Migliavacca, M. (2020). Nutrients and water availability constrain the seasonality of vegetation activity in a Mediterranean ecosystem. *Global Change Biology*, *26*(8), 4379–4400. https://doi.org/10.1111/gcb.15138

Luo, Y., El-Madany, T. S., Filippa, G., Ma, X., Ahrens, B., Carrara, A., Gonzalez-cascon, R., Cremonese, E., Galvagno, M., & Tiana, W. (2018). Using Near-Infrared-Enabled Digital Repeat Photography to Track Structural and Physiological Phenology in

Mediterranean Tree – Grass Ecosystems. *Remote Sensing*, *10*, 1293. https://doi.org/10.3390/rs10081293

Nair, R. K. F., Morris, K. A., Hertel, M., Luo, Y., Moreno, G., Reichstein, M., Schrumpf, M., & Migliavacca, M. (2019). N:P stoichiometry and habitat effects on Mediterranean savanna seasonal root dynamics. *Biogeosciences*, *16*(9), 1883–1901. https://doi.org/10.5194/bg-16-1883-2019

Nijland, W., de Jong, R., de Jong, S. M., Wulder, M. A., Bater, C. W., & Coops, N. C. (2014). Monitoring plant condition and phenology using infrared sensitive consumer grade digital cameras. *Agricultural and Forest Meteorology*, *184*, 98–106. https://doi.org/10.1016/j.agrformet.2013.09.007

Pedersen, E. J., Miller, D. L., Simpson, G. L., & Ross, N. (2019). Hierarchical generalized additive models in ecology: An introduction with mgcv. *PeerJ*, *7*, e6876. https://doi.org/10.7717/peerj.6876

Poorter, H., Bühler, J., van Dusschoten, D., Jos Climent, & Postma, Johannes A. (2012). Pot size matters: A meta-analysis of the effects of rooting volume on plant growth. *Functional Plant Biology*, *39*, 839–850. https://doi.org/10.1071/FP12049.

R Core Team. (2018). *R: A Language and Environment for Statistical Computing*.

Radville, L., McCormack, M. L., Post, E., & Eissenstat, D. M. (2016). Root Phenology in a Changing Climate. *Journal of Experimental Botany*, *67*(12), erw062-. https://doi.org/10.1093/jxb/erw062

Rahman, G., Sohag, H., Chowdhury, R., Wahid, K. A., Dinh, A., Arcand, M., & Vail, S. (2020). SoilCam: A Fully Automated Minirhizotron using Multispectral Imaging for Root Activity Monitoring. *Sensors*, *20*(3), 787. https://doi.org/10.3390/s20030787

Rahmanzadeh, H., & Shojaedini, S. V. (2016). *Novel Automated Method for Minirhizotron Image Analysis: Root Detection Using Curvelet Transform*. *29*(03), 337–346.

Raupach, M. R., Canadell, J. G., Ciais, P., Friedlingstein, P., Rayner, P. J., & Trudinger, C. M. (2011). The Relationship between Peak Warming and Cumulative CO2 Emissions, and Its Use to Quantify Vulnerabilities in the Carbon-Climate-Human

System. *Tellus, Series B: Chemical and Physical Meteorology*, *63*(2), 145–164. https://doi.org/10.1111/j.1600-0889.2010.00521.x

Richardson, A. D., Hufkens, K., Milliman, T., Aubrecht, D. M., Chen, M., Gray, J. M., Johnston, M. R., Keenan, T. F., Klosterman, S. T., Kosmala, M., Melaas, E. K., Friedl, M. A., & Frolking, S. (2018). Tracking Vegetation Phenology across Diverse North American Biomes Using PhenoCam Imagery. *Scientific Data*, *5*, 1–24. https://doi.org/10.1038/sdata.2018.28

Richardson, A. D., Keenan, T. F., Migliavacca, M., Ryu, Y., Sonnentag, O., & Toomey, M. (2013). Climate change, phenology, and phenological control of vegetation feedbacks to the climate system. *Agricultural and Forest Meteorology*, *169*, 156–173. https://doi.org/10.1016/j.agrformet.2012.09.012

Rytter, R.-M., & Rytter, L. (2012). Quantitative estimates of root densities at minirhizotrons differ from those in the bulk soil. *Plant and Soil*, *350*(1), 205–220. https://doi.org/10.1007/s11104-011-0896-6

Sloan, V. L., Fletcher, B. J., & Phoenix, G. K. (2016). Contrasting synchrony in root and leaf phenology across multiple sub-Arctic plant communities. *Journal of Ecology*, *104*(1), 239–248. https://doi.org/10.1111/1365-2745.12506

Smith, A. G., Han, E., Petersen, J., Olsen, N. A. F., Giese, C., Athmann, M., Dresbøll, D. B., & Thorup-Kristensen, K. (2020). RootPainter: Deep Learning Segmentation of Biological Images with Corrective Annotation. *BioRxiv*, 2020.04.16.044461. https://doi.org/10.1101/2020.04.16.044461

Sonnentag, O., Hufkens, K., Teshera-Sterne, C., Young, A. M., Friedl, M., Braswell, B. H., Milliman, T., O'Keefe, J., & Richardson, A. D. (2012). Digital Repeat Photography for Phenological Research in Forest Ecosystems. *Agricultural and Forest Meteorology*, *152*(1), 159–177. https://doi.org/10.1016/j.agrformet.2011.09.009

Steinaker, D. F., Wilson, S. D., & Peltzer, D. A. (2010). Asynchronicity in Root and Shoot Phenology in Grasses and Woody Plants. *Global Change Biology*, *16*(8), 2241–2251. https://doi.org/10.1111/j.1365-2486.2009.02065.x

Sullivan, P. F., & Welker, J. M. (2005). Warming chambers stimulate early season growth of an arctic sedge: Results of a minirhizotron field study. *Oecologia*, *142*(4), 616–626. https://doi.org/10.1007/s00442-004-1764-3

Svane, S. F., Dam, E. B., Carstensen, J. M., & Thorup-Kristensen, K. (2019). A multispectral camera system for automated minirhizotron image analysis. *Plant and Soil*, *441*, 657–672. https://doi.org/10.1007/s11104-019-04132-8

Taylor, B. N., Beidler, K. V., Strand, A. E., & Pritchard, S. G. (2014). Improved Scaling of Minirhizotron Data Using an Empirically-Derived Depth of Field and Correcting for the Underestimation of Root Diameters. *Plant and Soil*, *374*(1–2), 941–948. https://doi.org/10.1007/s11104-013-1930-7

The GIMP Development Team. (2019). *GIMP*. https://www.gimp.org

Upchurch, D. R., & Ritchie, J. T. (1984). *Battery-Operated Color Video Camera for Root Observations in Mini-Rhizotrons*. 1015–1017.

Vamerali, T., Ganis, A., & Mosca, G. (2009). *Methods For Thresholding Minirhizotron Root Images*. *September*, 1–2.

Vincent, C., Rowland, D., Na, C., & Schaffer, B. (2016). A High-Throughput Method to Quantify Root Hair Area in Digital Images Taken in Situ. *Plant and Soil*. https://doi.org/10.1007/s11104-016-3016-9

Wang, T., Rostamza, M., Song, Z., Wang, L., McNickle, G., Iyer-Pascuzzi, A. S., Qiu, Z., & Jin, J. (2019). SegRoot: A high throughput segmentation method for root image analysis. *Computers and Electronics in Agriculture*, *162*, 845–854. https://doi.org/10.1016/j.compag.2019.05.017

Yang, Y., Hillebrand, H., Lagisz, M., Cleasby, I., & Nakagawa, S. (n.d.). Low statistical power and overestimated anthropogenic impacts, exacerbated by publication bias, dominate field studies in global change biology. *Global Change Biology*, *n/a*(n/a). https://doi.org/10.1111/gcb.15972